Syed Qummer Zia Gilani[1,2,*]
Jakub Wiener[2]
M. Salman Naeem[1]
Zafar Javed[1]
Abdul Jabbar[1]
Hafiz Affan Abid[1]
Mehmet Karahan[3,*] (ID)

[1] National Textile University Faisalabad,
Faculty of Engineering and Technology,
Pakistan,
* e-mail: qummerzia@gmail.com

[2] Technical University of Liberec,
Faculty of Textile Engineering,
Czech Republic

[3] Bursa Uludağ University,
Vocational School of Technical Sciences,
Görükle-Bursa, Turkey,
* e-mail: mkarahan@uludag.edu.tr

# Adsorption Kinetics of an Activated Carbon Glass Composite Prepared Using Acrylic Waste Through Laser Treatment

**DOI:** 10.5604/01.3001.0014.8234

## Abstract

*This work explains a novel method of producing activated carbon using laser treatment. Acrylic coated glass samples were developed by padding a glass non-woven sheet in 30% acrylic fibre solution (PAN solution) from waste acrylic bathmats. Samples were then dried and cured at different temperatures. After curing, stabilisation was performed at 230 °C with a heating rate of 50 °C hr⁻¹. Infrared laser irradiation was performed on the stabilised web using a commercial pulsed infrared laser for carbonisation. The resultant acrylic glass carbon composite (AGCC) was characterised with the help of x-ray diffraction analysis, energy dispersive w-ray, and a scanning electron microscope to determine the increase in crystallinity as well as the percentage of carbon and surface roughness of the carbon glass composites. The adsorption capacity of the activated carbon (AC) glass composite prepared was determined by changing process inputs like the concentration of dye, the amount of AC glass composite, the agitation speed and pH. The results were analysed through different adsorption isotherms. It was established that the Freundlich model can more effectively describe results due to the development of heterogeneous surface characteristics. The kinetics of adsorption were studied using first order and second order models.*

**Key words:** *acrylic, heating rate, activated carbon, adsorption, stabilisation, carbonisation.*

## Introduction

The textile sector is a main contributor to the economies of many developing countries around the world. Although this sector is helping these countries to boost their economies, at the same time it is responsible for serious environmental concerns, such as air and water pollution. This situation has been further aggravated because of excessive use of synthetic dyes, as these dyes offer low cost and a vast variety of colors in comparison with natural dyes [1]. However, the presence of an aromatic structure in synthetic dyes makes them resistant to degradation through physical and chemical means. On the other hand, dye usage is increasing because of higher demand in the leather, denim, tanning, home textiles and paper production industries [2]. Around 10.000 kinds of synthetic dyes are being used in different manufacturing industries, out of which 20% of these are wasted as unused because of process inefficiencies [3]. There are different types and varieties of synthetic dyes in use, like reactive dyes, basic dyes, direct dyes etc. Dye removal from wastewater depends on different parameters, such as the method of dye removal, dye concentration and the solubility of dye. Methylene blue is a water-soluble dye generally used in the dying of silk, acrylic and cotton textiles. The excess amount of methylene blue in water is responsible for serious health hazards, and thus its removal from textile waste effluents is highly recommended [4].

Currently, different techniques are employed for the exclusion of dyes and other hazardous elements from wastewater like physical, chemical and biological methods. Biological methods are not helpful in removing synthetic dyes from textile effluents. On the other hand, chemical methods are highly expensive, which increases the cost of the final product [1, 5]. In this scenario adsorption seems to be a favorable approach as this method is not only inexpensive, effective, simple and without the production of any hazardous chemicals but is also accompanied with higher removal of adsorbate. For physical adsorption, different adsorbent materials having a porous structure and higher surface area are used [6]. Activated carbon (AC) is a famous adsorbent which is used for the adsorption of different chemicals, volatile organic compounds (VOC), gases and odours [7, 8]. Around 80% of activated carbon is used in water filtration, with the remaining used in air filtration and other applications such as odour adsorption, as well as in the pharmaceuticals, food processing and chemical industry [9]. Activated carbon is a microcrystalline form of carbon which is characterised by a higher surface area, porosity, heterogeneous elements, as well as different functional groups [10]. All these attributes make activated carbon an excellent adsorbent to be used for adsorption purposes. Activated carbon is developed in different forms like granular, powder and activated carbon cloth, but more recently the trend is now shifting towards the development of activated carbon non-woven webs [11, 12]. Practically, carbon rich materials can be used for the development of activated carbon. Out of the different precursors, polyacrylonitrile appears to be promising because of its higher yield, greater porosity, and surface area.

Depending upon the end usage, different techniques are being employed for the development of activated carbon [13]. These methods have some advantages as well as some limitations. The chemical method of producing activated carbon is not environmentally friendly; however, a higher surface area is achieved. In the physical method, higher energy is required to reach higher temperature during carbonisation, but less surface area is achieved as compared to the chemical method of activation [14]. In this study, acrylic fibres from textile waste were dissolved in solvent to make acrylic fibre solution (acrylic solution), which was then applied on glass fibre nonwoven sheets to prepare acrylic glass composite sheets. The sample prepared was stabilised in the presence of air at a slow heating rate for complete stabilisation, after which the material was carbonised using high temperature laser treatment. The AC glass composite prepared was charac-
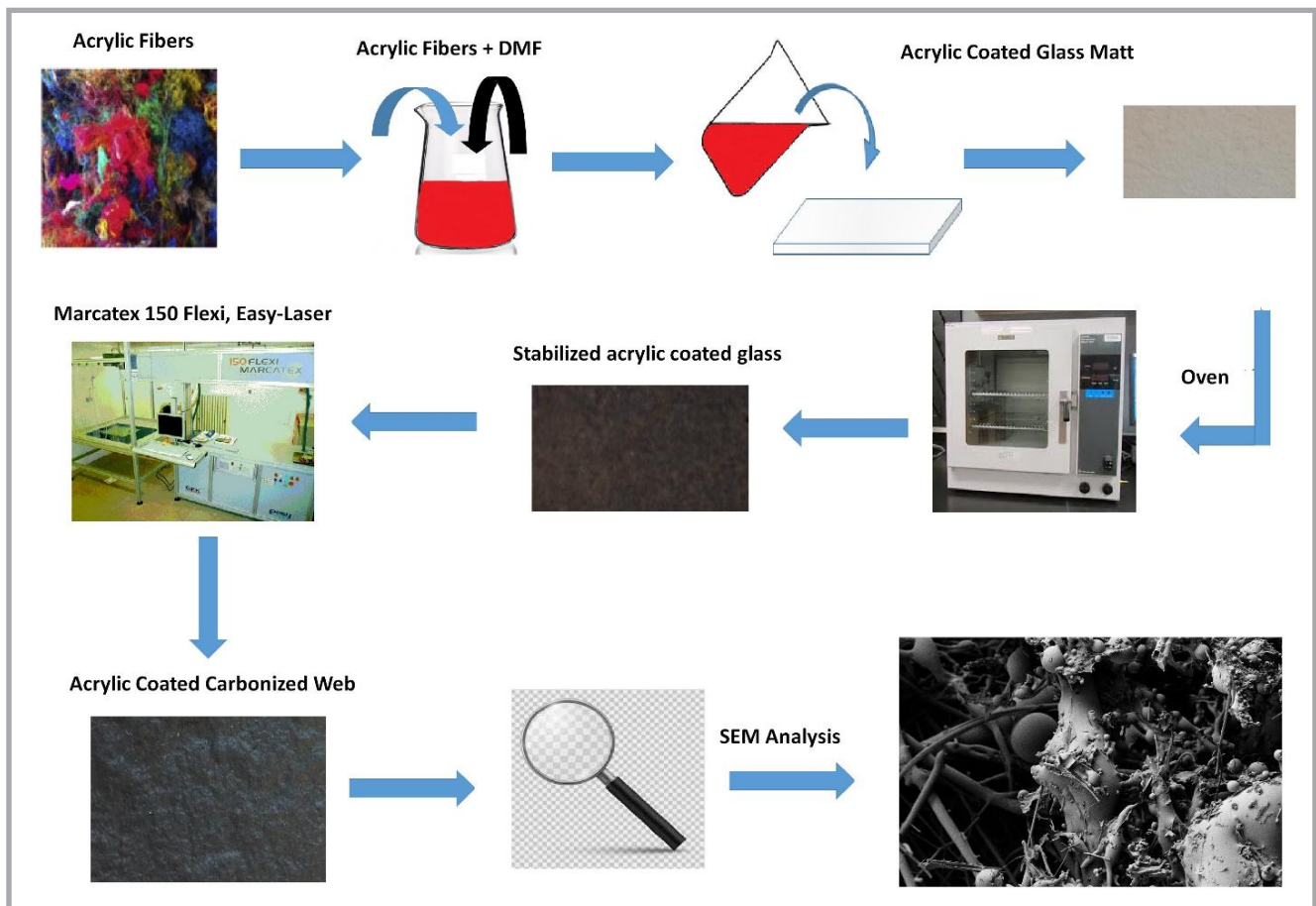
***Figure 1.*** *Schematic diagram of the formation of carbonised acrylic coated glass.*

terised using different characterisation techniques. Furthermore, the adsorption capability of the AC glass composite prepared was determined using methylene blue at different process parameters.

## ■ Material and methods

### Materials

Acrylic fibrous waste was provided by Grund s.r.o, Czech Republic. Glass nonwoven sheets were supplied by Specialni Papirenske Technologies (SEPAT), Czech Republic. Dimethyl Formamide (DMF) was provided by Sigma Aldrich, Czech Republic for dissolving polyacrylonitrile (PAN), as acrylic fibres are spun from PAN polymer. Details of acrylic fibre characteristics can be seen from ***Table 1***.

### Preparation of acrylic glass composite

Acrylic coated glass samples were made by padding glass nonwoven sheets in acrylic fibre solution (PAN solution). The acrylic fibres were then cleaned, washed, and dried at 100 °C until they became dry. The dried fibres were dissolved in DMF. A PAN solution of 30% by weight of acrylic was prepared to further increase the concentration of acrylic in the solvent, leading to an increase in solution viscosity. When the concentration of acrylic was increased to 30%, it became too thick to be used for padding or coating. Nonwoven glass fibre sheets were padded in this polymer solution with a 100% pickup. Acrylic coated glass mat samples were developed using the pad-dry-cure process. Samples were dried at 100 °C for 2 minutes and then cured at 160 °C for 4 minutes.

### Heat stability of acrylic-glass composites

Acrylic coated samples were first stabilised so that they could withstand higher carbonisation temperature during laser treatment. The initial weight of samples ($W_1$) before heat stabilisation was determined using an electric weighing balance. These samples were stabilised at 230, 280 and 330 °C in a muffle furnace at 50 °C hr$^{-1}$. After completion of the heat treatment, the stabilised sheet was removed from the furnace. The final weight $W_2$ of the sample was determined using the electrical balance, and weight loss $W_L$ calculations were made using ***Equation (1)***:

$$W_L(\%) = (W_1 - W_2) *100/W_1 \qquad (1)$$

### Carbonisation of stabilised acrylic-glass composites

Carbonisation was performed using an infrared laser (Marcatex 150 Flexi, Easy-Laser), which produced a high temperature IR pulsed laser with a wavelength of 10.6 μm. Different parameters such as the speed of the laser (bits/ms), the duty cycle (%), and frequency [kHz]

***Table 1.*** *Characteristics of acrylic fibres.*

| Sr. No. | Characteristics of acrylic fibres | |
|---|---|---|
| 1 | Acrylic monomer, % | 87 |
| 2 | Fineness, Den | 12 |
| 3 | Elongation, % | 43 |
| 4 | Shrinkage, % | 2.6 |

determine the power of the laser or how much temperature the laser is producing at the striking point. Optimised settings of these parameters and the temperature required of the stabilised material can be achieved. A lower value of the marking speed presents a longer marking time. During the process of laser treatment, the marking speed of the laser beam was set at 8 bits/ms and the duty cycle (DC) at 50%. The laser power used was 100 W at 50% of DC and 5 kHz. *Figure 1* shows a schematic diagram of the formation of the acrylic glass composite.

## Characterisation of AC glass composites

### SEM morphology

The morphology of the AC glass composite was analysed using a scanning electron microscope. This technique helped us to investigate change in the surface characteristics of the AC glass composite after carbonisation. Micrographic images were obtained at 1000x magnification at 2 kV voltage. There was no need for gold coating before scanning the glass composite as the samples developed were electrically conductive.

### Energy dispersive x-ray (EDX) analysis

The proportion of different elements like carbon, oxygen and others was determined by EDX analysis, conducted using Oxford Instruments.

### X-ray diffraction (XRD) analysis

XRD analysis was performed using a Malvern PAN analytical machine with a copper anode source. This analysis was helpful in determining crystalline as well as amorphous regions in glass carbon composites. The XRD technique is also useful for determining the crystallinity in material, the distance between carbon basal planes, and unit cell dimensions. The rise in crystallinity because of the application of heat can be determined using *Equation (2)*.

$$I_c = 1 - \frac{I_1}{I_2} \qquad (2)$$

Where, $I_1$ and $I_2$ correspond to the intensity at minimum and maximum peaks [15].

### Adsorption of carbon glass composite (CGC) for the removal of methylene blue

Methylene blue was used for evaluating the adsorption characteristics of a carbon glass composite (CGC) that had been

stabilised at 230 °C at a heating rate of 5 °C hr$^{-1}$ and laser irradiated at 6 bits m$^{-1}$ sec$^{-1}$. Methylene blue with different concentrations from 3 mg l$^{-1}$ to 15 mg l$^{-1}$ was prepared in distilled water. The adsorption performance was calculated using the batch method. A definite quantity of dye solution (50 ml) was added to different flasks, and a pre-weighed amount of adsorbent (carbon glass composite) was added to the dye solutions. The flasks, having different concentrations of dye solutions and a fixed amount of adsorbent, were put in a bath shaker for 180 minutes at 200 rpm to reach the equilibrium point. From these flasks, dye solutions were taken out after every 20 minutes, and the concentration of remaining dye was checked with the help of a spectrometer (UV-1600 pc spectrophotometer) at 665.0 nm. The adsorption performance of the adsorbent was also checked at different adsorbent dosages by varying the adsorbent quantity from 0.5 mg l$^{-1}$ to 2.5 mg l$^{-1}$. The effect of the stirring speed was also determined by changing the speed of the water bath shaker from the stationary position to 200 rpm while keeping other factors (amount of dye in the aqueous solution, quantity of carbon composite used etc.) constant. As dye water contains different surfactants, additives and other impurities, which causes variation in wastewater, the effect of pH on the adsorption performance was calculated at different pH. Dye removal from the aqueous solution was determined using *Equation (3)*.

$$Dye\ removal\ (\%) = \left[\frac{C_o - C_e}{C_o}\right] \times 100 \qquad (3)$$

Here, $C_o$ (mg l$^{-1}$) represents the initial dye concentration without the addition of adsorbent while $C_e$ (mg l$^{-1}$) stands for the final concentration of dye after completion of the adsorption process. The adsorption performance of the AC glass composite was calculated using the following *Equation (4)*.

$$q_e = (C_o - C_e)\frac{V}{W} \qquad (4)$$

Where, $q_e$ (mg g$^{-1}$) represents dye adsorbed on the adsorbent, $W$ (g) the amount of adsorbent, and $V$ (liters) is the volume of the solution.

## Adsorption isotherms

Adsorption isotherms helped to understand the principle of adsorption like how dye molecules are adsorbed on the AC glass composite, and in-liquid media

till equilibrium was established. Both Langmuir and Freundlich adsorption isotherms helped to understand the adsorption mechanism.

### Langmuir isotherm

According to this model, dye molecules are adsorbed at homogenous sites of the AC glass composite in the form of monolayer adsorption on the adsorbent. The general equation of the Langmuir model is shown in *Equation (5)* [16].

$$q_e = \frac{q_{max}K_L C_e}{1 + K_L C_e} \qquad (5)$$

Where, $q_{max}$ represent the maximum dye adsorbed (mg g$^{-1}$), $C_e$ the concentration of dye (mg l$^{-1}$), and $K_L$ (lm g$^{-1}$) stands for the rate of adsorption.

### Freundlich isotherm

According to the Freundlich model, the surface of the adsorbent is heterogeneous in terms of porosity, surface functional groups and other adsorption sites. This model considers the heterogeneity of the adsorbent surface and confirms multilayer adsorption on the adsorbent surface. The general equation of the Freundlich isotherm is shown in *Equation (6)* [17].

$$q_e = K_F C_e^{1/n} \qquad (6)$$

Where, $K_F$ is the Freundlich constant, showing the capacity of adsorption (mg g$^{-1}$), $C_e$ for the dye concentration, and 1/n represents the intensity of adsorption on the adsorbent (lm g$^{-1}$).

## Adsorption kinetics

The kinetics of the reaction were investigated using first and second order reactions. The general form of the first order reaction can be seen in *Equation (7)*.

$$q_t = q_e(1 - exp^{-K_1 t}) \qquad (7)$$

Where, $K_1$ represent the equilibrium constant for the rate of adsorption (min$^{-1}$), $q_t$ and $q_e$ shows the amounts of adsorbate accumulated on the AC glass composite at any time (min) and after the reaction reached equilibrium. The general form of the Pseudo first order after linearisation can be seen in following *Equation (8)*.

$$\log(q_e - q_t) = \log q_e - \frac{K_1 t}{2.303} \qquad (8)$$

While the general and linear form second order reactions are shown in *Equations (9)* and *(10)*.

$$q_t = \frac{K_2 q_e^2 t}{1 + K_2 t} \qquad (9)$$

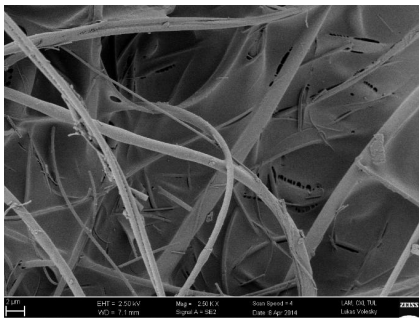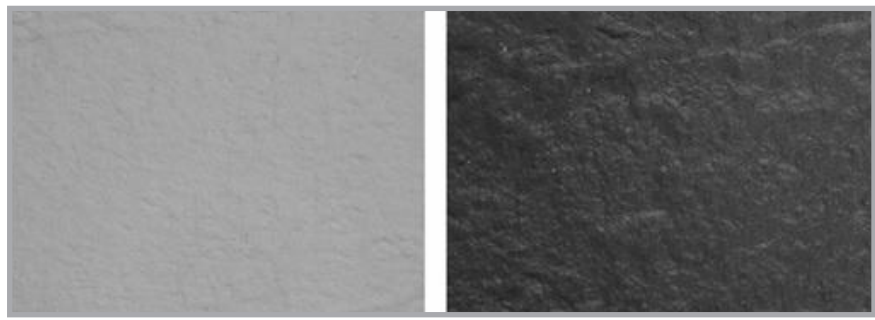*Figure 2.* SEM image of acrylic coated glass (ACG).



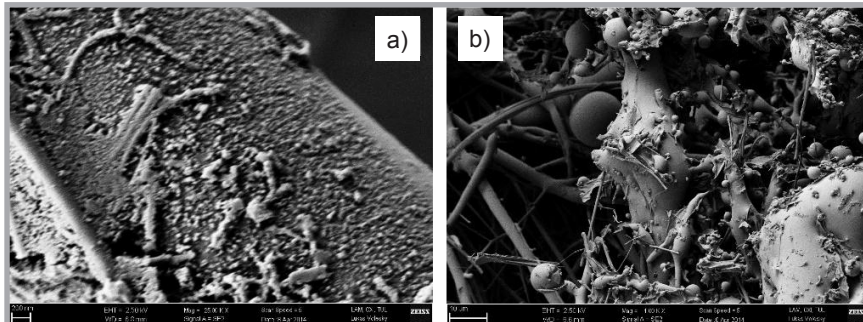*Figure 3.* Image of acrylic coated glass and stabilised acrylic coated glass.



*Figure 4.* SEM image of carbon glass composite.

Here, $K_2$ represents the equilibrium constant for the rate of adsorption (min$^{-1}$).

$$\frac{t}{q_t} = \frac{1}{K_2 q_e^2} + \frac{t}{q_e} \qquad (10)$$

## ■ Results and discussion

### Effect of stabilisation and laser treatment

An AC glass composite was prepared by heat stabilisation in a muffle furnace and carbonisation through laser treatment. Acrylic solution was deposited as a thin layer on the glass sheet. The glass fibres in the sheet only served as base material for the deposition of acrylic. Later, the acrylic coated glass sheet was initially dried at 100 °C and cured at 160 °C to avoid heat shock, which can cause different problems like bubble formation or tearing away of the unstabilised layer. To ensure proper stabilisation, a slow heating rate of 50 °Chr$^{-1}$ was selected. The stabilisation was conducted at 230, 280 and 330 °C. It was found that as the

stabilisation temperature was increased, there was a gradual loss of yield due to more elimination of different elements in the form of different gases, as can be seen from *Table 2* [18].

The stabilised sample prepared at 230 °C exhibited minimum weight loss and was selected for further carbonisation processing. The slow heating rate during stabilisation helped to form a stabilised layer without bubbles, as can be seen from *Figure 2*.

The black colour after stabilisation (at 230 °C) indicated that proper stabilisation was achieved, as explained in *Figure 3*.

Since laser is a pointing treatment that causes an instantaneous local heating phenomenon in the sample instead of the complete heating of the material, the stabilised acrylic coated glass was later laser irradiated at a lower marking speed. The low marking speed during laser treatment ensured high

temperature, especially at the point of laser striking. Such high local heating for stabilised acrylic coated glass was sufficient to cause carbonisation in the sample.

### SEM analysis

SEM analysis showed that high temperature during laser irradiation caused surface roughness, as shown in *Figure 4.a*. The surface roughness can be due to the removal of different functional groups, leading to the development of a carbon structure or arrangement of carbon chains by carbonisation. The increased surface roughness after laser irradiation, which indicates an increase in the surface area. was around 275 m$^2$/g [19]. The small packets in the developed carbon surface, shown in *Figure 4.b*, are because of entrapped gasses which are released during local heating.

### EDX analysis

This analysis was conducted after laser irradiation to determine the proportion of different elements in the AC glass composite. It was found that after laser irradiation the carbon content had increased to 93.39%, while the content of oxygen was found to be 5.24%. The higher temperature during laser heating caused the removal of other elements other than carbon, which caused a higher proportion of carbon after laser treatment, as shown in *Figure 5* [20].

### XRD analysis

To determining the degree of crystallinity and inter-planar distance, XRD analysis was performed. From *Figure 5* the XRD pattern of activated carbon prepared using laser treatment can be seen. This technique helped to determine the development of crystallinity and inter-planar spacing after laser treatment. Each element has a characteristic peak at a specific angle, and the literature shows that

*Table 2.* Weight loss of acrylic glass composites after heat treatment.

| Sample No. | Temp., °C | Initial weight, gm | Final weight, gm | Difference, gm | Weight loss, % |
|---|---|---|---|---|---|
| 1 | 230 | 1.09 | 0.907 | 0.183 | 16.79 |
| 2 | 280 | 0.751 | 0.613 | 0.138 | 18.38 |
| 3 | 330 | 1.27 | 0.809 | 0.461 | 36.30 |

a peak around 26 degrees exhibits the presence of carbon in the structure. From the results of XRD, shown in *Figure 6*, it was found that the peak obtained at 26.33° confirmed the presence of carbon after laser treatment [21]. The literature also showed that the degree of crystallinity can be determined from the nature of the peak exhibited by the XRD pattern. It was found using *Equation (2)* that 87.5% crystallinity was achieved by the use of laser treatment along with 0.33 nm inter layer spacing.

**Application of AC glass composite for dye removal**

*Effect of stirring speed*

The effect of stirring speed on dye removal efficiency and adsorption capacity was determined while maintaining the methylene blue concentration at 9 mg l$^{-1}$, the temperature at 25 °C, the adsorbent dosage at 2 mg l$^{-1}$, and the contact time at 180 minutes to ensure maximum dye removal. One sample was kept without agitation, while the stirring speed was increased to 200 rpm for other samples. *Figure 7* shows that 3.1 % removal was achieved without agitation, while removal efficiency was increased from 38.75% to 56.58%, 72.09% and 82.17% when the stirring speed was gradually increased from 50 rpm to, 100, 150 and 200 rpm, respectively.

The dye accumulation capacity on the adsorbent was increased with an increase in the stirring speed. It increased from 0.13 mgg$^{-1}$ to 3.57 mgg$^{-1}$ at the higher stirring speed due to more interaction of dye particles with the laser irradiated adsorbent.
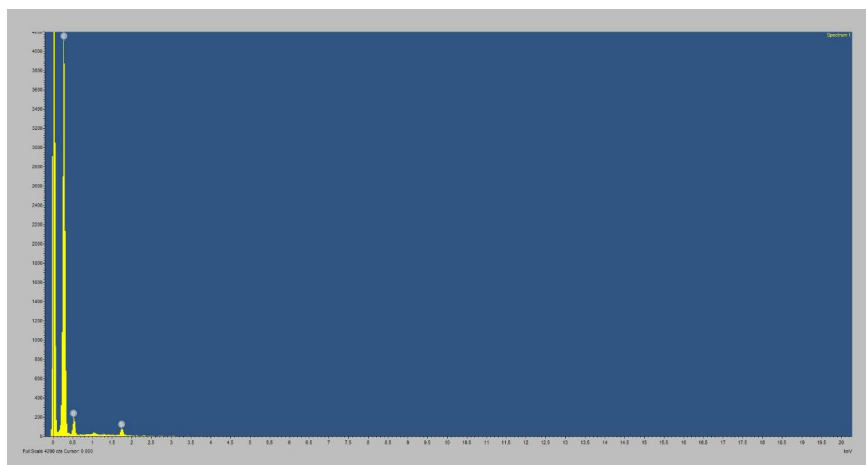


**Figure 5.** *EDX analysis of carbon glass composition.*

*Effect of dye concentration*

The effect of dye concentration on the removal percentage and adsorption capacity of the AC glass composite was checked by changing the dye concentration from 3 mgl$^{-1}$ to 15 mgl$^{-1}$ while other factors (adsorbent dosage ((0.1 gl$^{-1}$)) and stirring speed) were kept constant. *Figure 8* shows that the removal percentage increased with the passage of time till the process reached equilibrium. At lower dye concentration, the process reached equilibrium in less time due to the high availability of adsorption sites for adsorbate molecules [21]. However, more contact time is required to reach equilibrium at higher concentration because of the less availability of adsorption sites for dye molecules. At lower dye concentration, the process reached equilibrium in 120 minutes, which was jumped to 180 minutes at the higher concentration of dye. It was found that the dye removal percentage decreased from 93.2 to

75.67% when the concentration of dye was changed from 3 mgl$^{-1}$ to 15 mgl$^{-1}$, as shown in *Figure 8*.

The accumulation of dye on the AC glass composite increased with an increase in the dye concentration and passage of time till the process reached equilibrium. Similarly, the adsorption capacity was also increased by increasing the amount of dye in the solution. The adsorption performance increased from 1.41 mg g$^{-1}$ to 5.66 mg g$^{-1}$ when the concentration of dye was increased from 3 mg l$^{-1}$ to 15 mg l$^{-1}$, as can be seen from *Figure 9*, due to more availability of dye molecules per unit mass of the AC glass composite [22].

*Effect of adsorbent quantity*

To determine the effect of adsorbent quantity on the dye removal efficiency and adoption performance of the AC glass composite, its quantity was increased up to 5 mg l$^{-1}$. *Figure 10* shows that as the
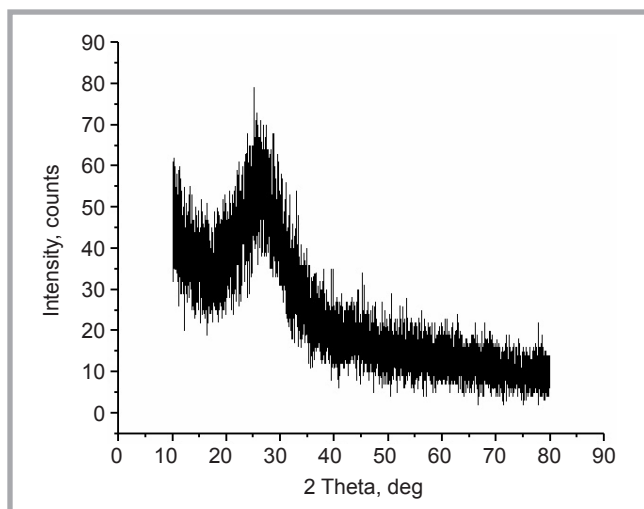


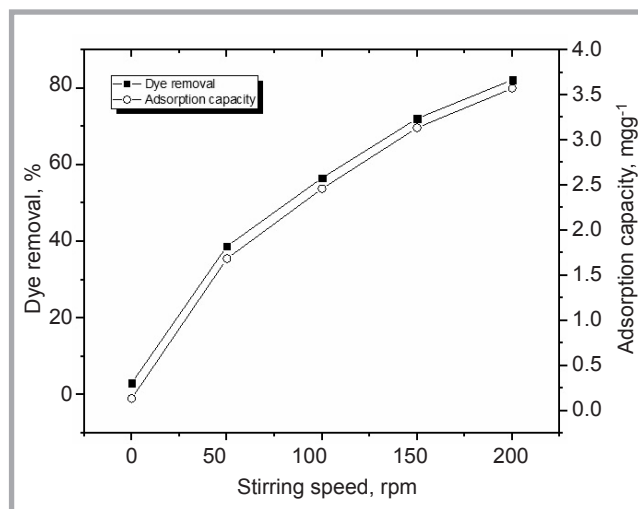**Figure 6.** *XRD pattern of acrylic coated glass carbon composite.*



**Figure 7.** *Effect of different stirring speeds on the dye removal efficiency and adsorption capacity of the carbon glass composite at 25 °C.*
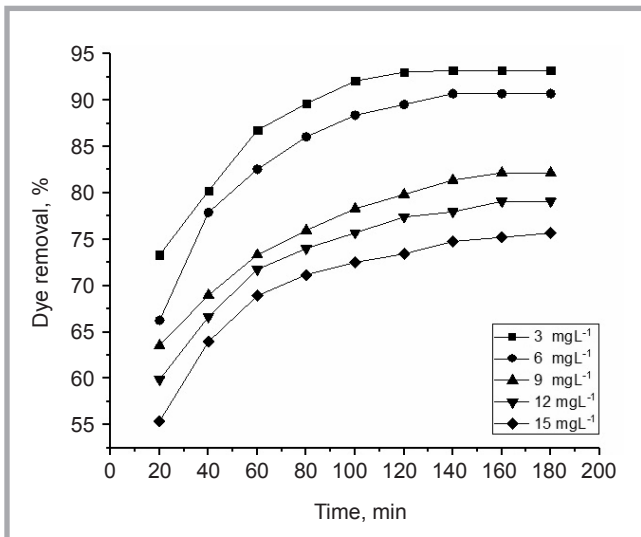
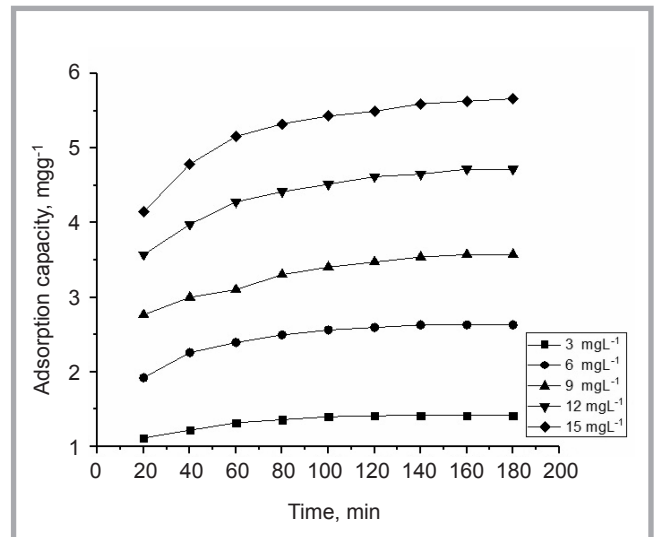**Figure 8.** *Effect of dye concentration on the dye removal efficiency of the carbon glass composite at 25 °C.*



**Figure 9.** *Effect of dye concentration on the adsorption capacity of the carbon glass composite at 25 °C.*
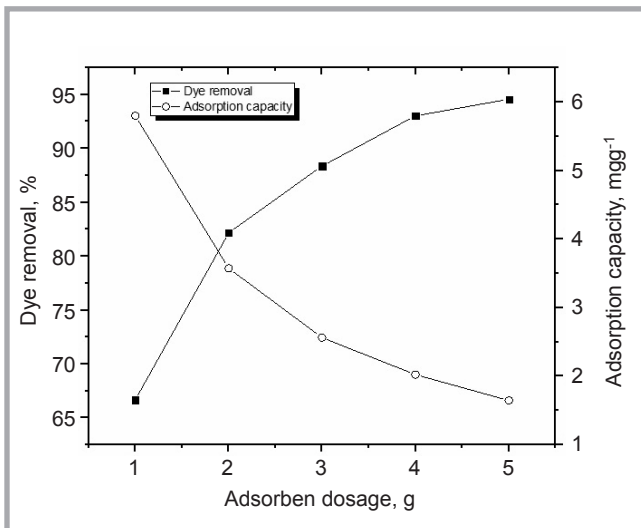


**Figure 10.** *Effect of adsorbent concentration on the dye removal and adsorption capacity of the carbon glass composite at 25 °C.*
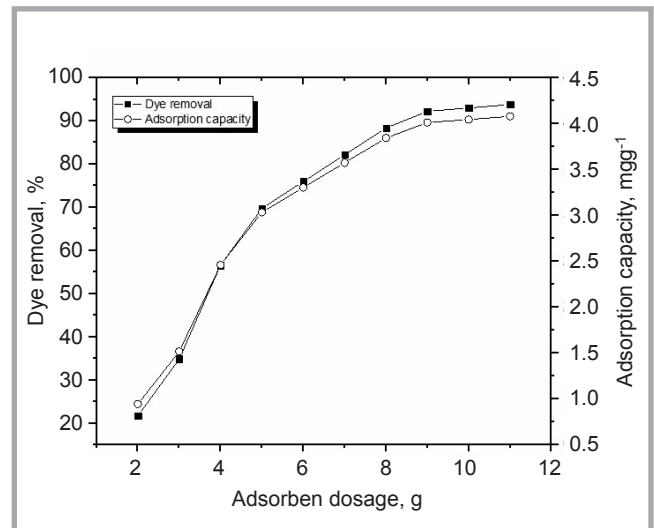


**Figure 11.** *Effect of pH on the dye removal and adsorption capacity of the carbon glass composite at 25 °C.*
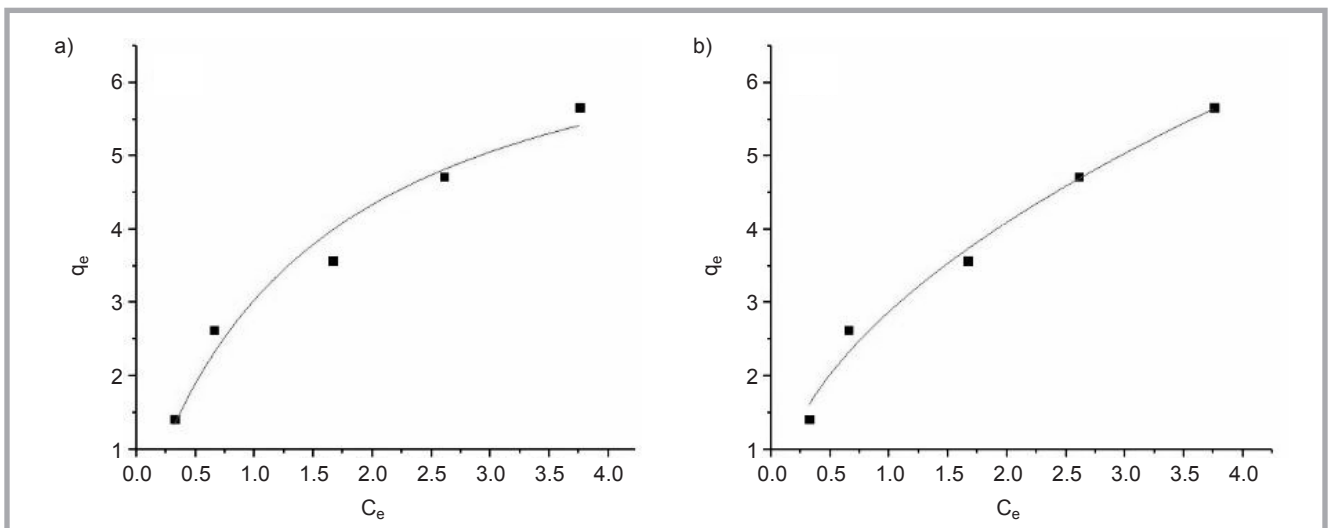


**Figure 12.** *a) Langmuir isotherm (non-linear), b) Freundlich isotherm (non-linear).*
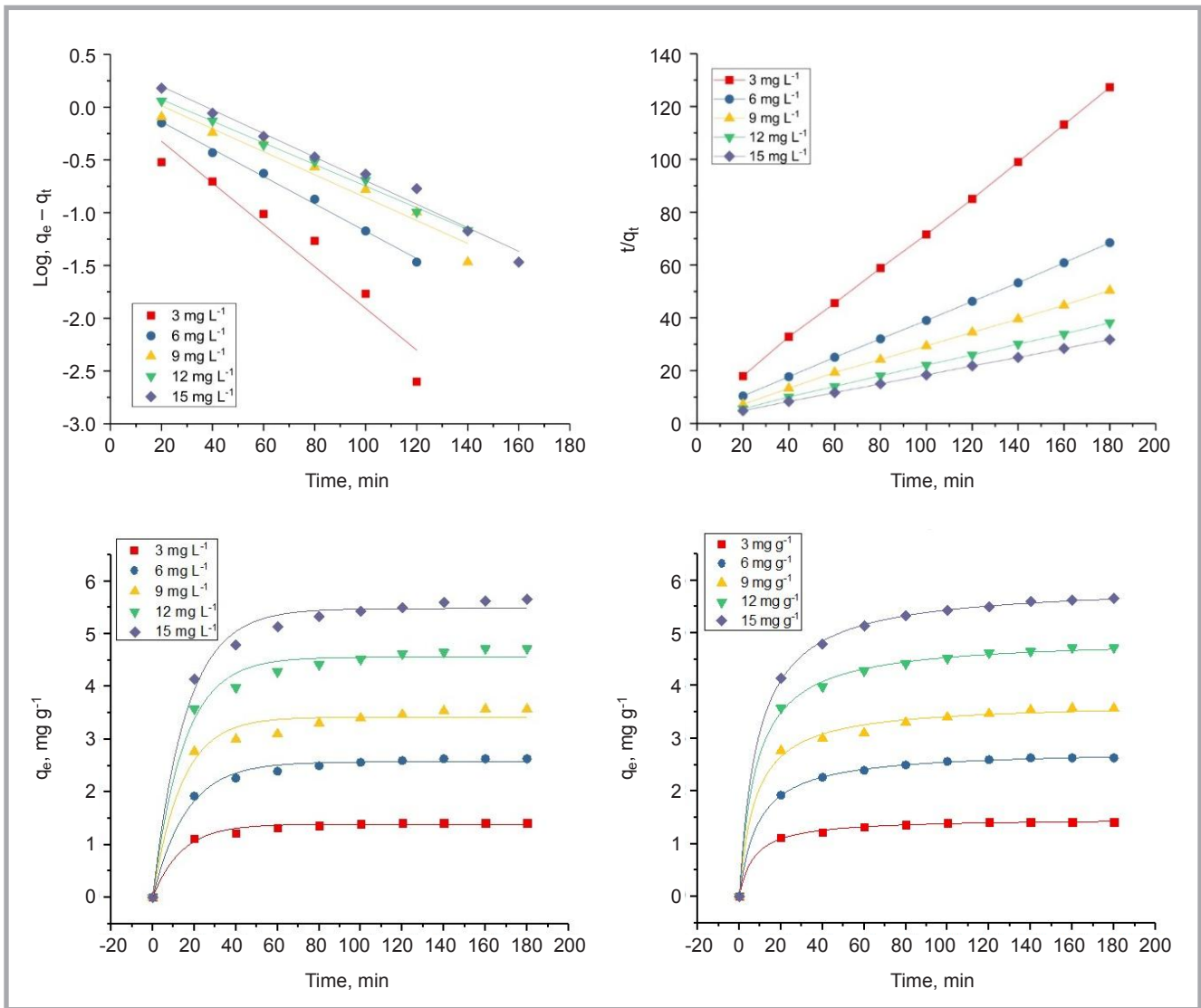
*Figure 13. Linear and non-linear model of first and second order.*

quantity of AC glass composite in the dye solution was increased from 1 mgl⁻¹ to 2 mgl⁻¹, 3 mgl⁻¹, 4 mgl⁻¹ and 5 mgl⁻¹, the dye removal percentage also increased from 66.66% to 82.17%, 88.37%, 93.02% and 94.57% respectively, due to the presence of a higher surface area and more adsorption sites at higher concentrations on the AC glass composite. The reverse trend was observed in the case of dye accumulation on the adsorbent, as shown in *Figure 9*. This was due to the fact that as the adsorbent quantity was increased, the adsorption sites remained unsaturated, which caused a reduction in the adsorption capacity [23, 24].

### Effect of pH on dye removal efficiency and adsorption capacity

pH has a significant effect on the adsorption process as it affects functional groups on the dye and adsorbent. To determine the effect of pH on the adsorp-

tion process, the pH of the solution was changed from 2 to 11 while keeping other factors (dye concentration, adsorbent dosage, temperature and stirring speed. of solution) constant at 25 °C. It can be observed from *Figure 11* that only 21.70% of dye was removed at pH 2. However, when the pH was increased from 3 to 11 gradually, there was a positive trend of dye removal from 34.88% to ultimately 93.79%. This is because the point of zero charge of the AC glass composite was at pH 5.9. Below this point, the surface of the AC glass composite became positively charged, while at higher pH the surface of carbon became negatively charged. Due to this reason, at a low pH the removal of methylene blue decreased because of the electrostatic repulsion of negatively charged dye particles and the positively charged surface of the AC glass composite. However, as the solution pH was increased, a positive

trend of dye removal and adsorption was observed because of the accumulation of negative charge on the AC glass composite, which caused more attraction of positively charged dye particles [25].

### Adsorption Isotherms
#### Langmuir isotherm

The Langmuir adsorption isotherm confirms the monolayer adsorption of adsorbate molecules on the adsorbent surface because the different functional groups or porosity present have uniform energies on the surface of the adsorbent [26]. A non-linear model of the Langmuir isotherm was drawn by placing $C_e$ on the x-axis versus the adsorption capacity ($q_e$). The dimensionless equilibrium number ($R_L$) was determined using *Equation (11)*, and the thin parameter was used for determining the characteristics of the Langmuir curve, as can be seen from *Table 3*.

**Table 3.** *Parameters for Langmuir isotherm.*

| $R_L = 0$ | Irreversible |
|---|---|
| $R_L = 1$ | Linear |
| $R_L > 1$ | Unfavourable |
| $0 < R_L < 1$ | Favourable |

**Table 4.** *Adsorption characteristics of Langmuir and Freundlich isotherms.*

| Langmuir adsorption isotherm | |
|---|---|
| $q_{max}$, mg g$^{-1}$ | $7.56 \pm 0.93$ |
| $K_L$, L mg$^{-1}$ | $0.672 \pm 0.20$ |
| $R_L$ | $0.67 \pm 0.20$ |
| $R^2$ | 0.968 |
| **Freundlich adsorption isotherm** | |
| $K_F$, mg g$^{-1}$ | $2.88 \pm 0.13$ |
| $1/n$, L mg$^{-1}$ | $0.50 \pm 0.17$ |
| $R^2$ | 0.985 |

$$R_L = \frac{1}{1+K_L C_o} \qquad (11)$$

The value of $R_L$, as predicted by the Langmuir model, was $0.67 \pm 0.20$, which means favourable adsorption of methylene blue on the AC glass composite. Non-linear curve fitting of the Langmuir isotherm gave the Langmuir constant for the adsorption rate ($K_L$) and maximum adsorption capacity ($q_{max}$). Non-linear models of the Langmuir and Freundlich isotherms were plotted, shown in *Figures 12.a* and *12.b*. The higher coefficient of determination (97.01%) shows that the experimental results of adsorption can be more accurately explained by the Langmuir model. The maximum dye adsorption capacity ($q_{max}$) on the AC glass composite was found to be $7.56 \pm 0.93$ mgg$^{-1}$, shown in *Table 4*.

### Freundlich isotherm

As compared to the Langmuir isotherm, The Freundlich isotherm focuses on heterogeneous surface characteristics of the adsorbent, which can be in the form of surface functional groups or adsorption sites [17]. The Freundlich isotherm relies on heterogeneous surface characteristics of the adsorbent in different aspects like the heterogeneous distribution of surface functional groups, uneven distribution of the porous structure, and the presence of disorganised carbon. Non-linear curve fitting of the Freundlich model was performed by placing $C_e$ (mg l$^{-1}$) on the x-axis while placing the adsorption capacity $q_e$ (mg g$^{-1}$) on the y-axis. From the intercept and slope of the Freundlich isotherm, the corresponding values of $K_F$ (adsorption capacity), $n$ (Freundlich constant for adsorption) and the coefficient of determination were calculated, given in *Table 4*. The higher value of $R^2$ confirmed that the non-linear form of the Freundlich model explained the adsorption mechanism on the carbon glass composite more precisely because of its heterogeneous surface characteristics. However, it is clear from *Table 4* that both isotherms can effectively be employed for understanding the adsorption mechanism in a AC glass composite.

### Adsorption kinetics

The adsorption kinetics helped to understand the mechanism of dye adsorption with the increasing contact time of the AC glass composite with methylene blue solution [27]. Dye accumulation on the carbon glass composite was determined through linear and nonlinear curve fitting of the first and second order reactions with the help of experimental results. The linear as well as non-linear curve fitting of both models were employed to find the results best suited with the experimental ones. Linear and non-linear curve fitting of the first order were determined by plotting log ($q_e$-$q_t$) versus time and adsorption capacity ($q_e$) at set intervals of time, as shown in *Figure 13*. However, curve fitting of the first and second order reactions was done by plotting t/$q_t$, adsorption capacity ($q_e$), against time, as shown in *Figure 13*.

From the intercept and slope of *Figure 13*, the adsorption capacity and reaction rate are calculated, shown in *Tables 5* and *6*. *Figure 13* shows that non-linear curve fitting of the first order reaction explains the results more accurately as compared to the linear model of the first order reaction. The non-linear model not only gave higher values of $R^2$ but also provided more accurate results of adsorption in relation to experimental results. Both linear models failed to explain the process of adsorption, while the non-linear models provided adsorption values very close to experimental results. Although the second order model gave a higher value of $R^2$ as compared to the non-linear model of the first order, the latter gave more accurate results of adsorption. Although there was only a slight difference between these models, the first order model more accurately explained the experimental values of adsorption. From the results, it can be concluded that the non-linear model of the first order can be more successfully employed for understanding the mechanism of adsorption on AC glass composites.

**Table 5.** *Parameters of pseudo first order of methylene blue adsorption on carbon glass composite.*

| Kinetic model parameters | Initial Concentrations (mgl$^{-1}$) | | | | |
|---|---|---|---|---|---|
| | 3 | 6 | 9 | 12 | 15 |
| $q_{e,exp}$ (mgg$^{-1}$) | 1.414 | 2.629 | 3.573 | 4.720 | 5.664 |
| **Linear model** | | | | | |
| $q_{e,cal}$, mgg$^{-1}$ | 0.072 | 0.119 | 0.231 | 0.278 | 0.421 |
| $K_1$, min | -0.019 | -0.012 | -0.010 | -0.010 | -0.011 |
| $R^2$ | 0.92 | 0.99 | 0.95 | 0.99 | 0.98 |
| **Non-linear model** | | | | | |
| $q_{e,cal}$, mgg$^{-1}$ | 1.386 | 2.570 | 3.420 | 4.559 | 5.481 |
| $K_1$, min | 0.072 | 0.062 | 0.071 | 0.067 | 0.063 |
| $R^2$ | 80.98 | 89.85 | 65.95 | 80.58 | 87.55 |

**Table 6.** *Parameters of pseudo second order of methylene blue adsorption on carbon glass composite.*

| Kinetic model parameters | Initial Concentrations (mgl$^{-1}$) | | | | |
|---|---|---|---|---|---|
| | 3 | 6 | 9 | 12 | 15 |
| $q_{e,exp}$, mgg$^{-1}$ | 1.414 | 2.629 | 3.573 | 4.720 | 5.664 |
| **Linear model** | | | | | |
| $q_{e,cal}$, mg g$^{-1}$ | 4.750 | 3.214 | 2.721 | 2.060 | 1.576 |
| $K_2$, min$^{-1}$ | 0.676 | 0.360 | 0.264 | 0.201 | 0.167 |
| $R^2$ | 0.99 | 0.99 | 0.99 | 0.99 | 0.99 |
| **Non-linear model** | | | | | |
| $q_{e,cal}$, mgg$^{-1}$ | 1.479 | 2.780 | 3.677 | 4.904 | 5.922 |
| $K_1$, min | 0.095 | 0.039 | 0.035 | 0.025 | 0.018 |
| $R^2$ | 97.15 | 99.66 | 91.55 | 97.96 | 99.59 |

### Desorption studies

A desorption study of activated carbon was performed using 1% NaOH. After 120 minutes of stirring at 200 rpm, it was found that 76% of methylene blue was desorbed from the surface of the developed activated carbon. The adsorption efficiency of the activated carbon was found to decrease gradually to 54% after three such desorption cycles.

### ■ Conclusions

In this study acrylic waste was effectively transformed into AC through laser irradiation. Acrylic based precursors are a preferred choice for producing AC because of higher yield and porosity; however, in the current study a unique approach for the development of AC glass composites was adopted. This method is novel in that acrylic was first dissolved in dimethyl formamide, which was then carbonised through laser treatment at high temperature. Acrylic solution was applied on a glass sheet, which provided a substrate for acrylic solution. The acrylic coated glass sample was stabilised at 230 °C at a slower heating rate. The stabilised material was carbonised with the help of a high temperature laser beam. The high temperature at the point source successfully converted the stabilised material into a AC glass composite. The XRD pattern confirmed the development of a carbon peak at 26°. The SEM image showed the development of a rough surface with a heterogeneous porous structure. The development of a heterogeneous surface made the AC glass composite favourable to be used for adsorption purposes. The adsorption characteristics of the AC glass composite were checked using methylene blue at different process parameters. The results show that higher contact time is required to reach equilibrium at high concentration. Furthermore, the adsorbent material shows higher adsorption at different levels of pH, adsorbent quantity and agitation speed. The results obtained were analysed, which showed that the Freundlich model more precisely explained the results because of the development of a heterogeneous surface after laser treatment. The outcomes of this study support the idea of the successful transformation of acrylic into AC using the novel approach of laser irradiation and its potential to be used for effluent treatment.

### References

1. Huang C-H, Chang K-P, Ou H-D, Chiang Y-C, Wang C-F. Adsorption of Cationic Dyes Onto Mesoporous Silica. *Microporous and Mesoporous Materials* 2011; 141(1-3): 102-109.
2. Qiu M, Huang C. Removal of dyes from aqueous solution by activated carbon from sewage sludge of the municipal wastewater treatment plant. *Desalination and Water Treatment* 2015; 53(13): 3641-3648.
3. Gupta V. Application of low-cost adsorbents for dye removal – a review. *Journal of environmental management,* 2009; 90(8): 2313-2342.
4. Ho Y-S, Malarvizhi R, Sulochana N. Equilibrium Isotherm Studies of Methylene Blue Adsorption onto Activated Carbon Prepared from Delonix Regia Pods. *Journal of Environmental Protection Science* 2009; 3: 111-116.
5. Naeem M S, Javed S, Baheti V, Wiener J, Javed M U, Hassan S Z U, Naeem J. Adsorption Kinetics of Acid Red on Activated Carbon Web Prepared from Acrylic Fibrous Waste. *Fibers and Polymers* 2018; 19(1): 71-81.
6. Sharma S, Bhattacharya A. Drinking water contamination and treatment techniques. *Applied Water Science* 2017; 7(3): 1043-1067.
7. Saini VK, Pires J. Development of Metal Organic Framework-199 Immobilized Zeolite Foam for Adsorption of Common Indoor Vocs. *Journal of Environmental Sciences* 2017; 55: 321-330.
8. Wang H, Wang B, Li J, Zhu T. Adsorption Equilibrium and Thermodynamics of Acetaldehyde/Acetone on Activated Carbon. *Separation and Purification Technology* 2019; 209*:* 535-541.
9. Chen J Y. *Activated Carbon Fiber and Textiles*: Woodhead Publishing, 2016.
10. Baheti V, Naeem S, Militky J, Okrasa M, Tomkova B. Optimized Preparation of Activated Carbon Nanoparticles from Acrylic Fibrous Wastes. *Fibers and Polymers* 2015; 16(10): 2193-2201.
11. Bansal R C, Goyal M. *Activated carbon adsorption*: CRC press, 2005.
12. Naeem S, Baheti V, Tunakova V, Militky J, Karthik D, Tomkova B. Development of Porous and Electrically Conductive Activated Carbon Web for Effective EMI Shielding Applications. *Carbon* 2017; 111: 439-447.
13. Zaini M A A, Amano Y, Machida M. Adsorption of Heavy Metals onto Activated Carbons Derived from Polyacrylonitrile Fiber. *Journal of Hazardous Materials* 2010; 180(1-3): 552-560.
14. Arami-Niya A, Daud W M A W, Mjalli F S. Comparative Study of the Textural Characteristics of Oil Palm Shell Activated Carbon Produced by Chemical and Physical Activation for Methane Adsorption. *Chemical Engineering Research and Design* 2011; 89(6): 657-664.
15. Siqueira G, Abdillahi H, Bras J, Dufresne A. High Reinforcing Capability Cellulose Nanocrystals Extracted from Syngonanthus Nitens (Capim Dourado). *Cellulose* 2010; 17(2): 289-298.
16. Langmuir I. The Adsorption of Gases on Plane Surfaces of Glass, Mica and Platinum. *Journal of the American Chemical Society* 1918; 40(9): 1361-1403.
17. Freundlich H. Über die Adsorption in Lösungen. *Zeitschrift f*ür Physikalische *Chemie* 1907; 57(1): 385-470.
18. Bhat G, Cook F, Abhiraman A, Peebles Jr L. New Aspects in the Stabilization of Acrylic Fibers for Carbon Fibers. *Carbon* 1990; 28(2-3): 377-385.
19. Yin X-w, Quan L. Effects of Heat Treatment Temperature on Microstructure and Electromagnetic Properties of Ordered Mesoporous Carbon. *Transactions of Nonferrous Metals Society of China* 2013; 23(6): 1652-1660.
20. Kim J-H, Jeong E, Lee Y-S. Preparation and Characterization of Graphite Foams. *Journal of Industrial and Engineering Chemistry* 2015; 32: 21-33.
21. Naeem S, Baheti V, Wiener J, Marek J. Removal of Methylene Blue from Aqueous Media Using Activated Carbon Web. *The Journal of The Textile Institute* 2017; 108(5); 803-811.
22. Chowdhury Z Z, Zain S M, Rashid A, Khalid K. Linear Regression Analysis for Kinetics and Isotherm Studies of Sorption of Manganese (II) Ions onto Activated Palm Ash from Waste Water. *Orient. J. Chem* 2011; 27(2): 405-415.
23. Crini G, Badot P. Sorption Processes and Pollution: Conventional and Non-conventional Sorbents for pollutant removal from Wastewaters, Presses Univ: Franche-Comté, 2010.
24. Secula MS, Cagnon B, Cretescu I, Diaconu M, Petrescu S. Removal of an Acid Dye from Aqueous Solutions by Adsorption on a Commercial Granular Activated Carbon: Equilibrium, Kinetic and Thermodynamic Study. *Scientific Study & Research. Chemistry & Chemical Engineering, Biotechnology, Food Industry* 2011; 12(4): 307.
25. Shah I, Adnan R, Ngah W S W, Mohamed N, Taufiq-Yap Y H. A New Insight to the Physical Interpretation of Activated Carbon and Iron Doped Carbon Material: Sorption Affinity Towards Organic Dye. *Bioresource Technology* 2014; 160, 52-56.
26. Baccar R, Blánquez P, Bouzid J, Feki M, Sarrà M. Equilibrium, Thermodynamic and Kinetic Studies on Adsorption of Commercial Dye by Activated Carbon Derived From Olive-Waste Cakes. *Chemical Engineering Journal* 2010; 165(2): 457-464.
27. Demirbas A. Oil from Tea Seed by Supercritical Fluid Extraction. *Energy Sources, Part A* 2009; 31(3): 217-222.